J Antimicrob Chemother 2022; **77**: 2718–2728
https://doi.org/10.1093/jac/dkac225 Advance Access publication 18 July 2022

Journal of Antimicrobial Chemotherapy

Population pharmacokinetics of apramycin from first-in-human plasma and urine data to support prediction of efficacious dose

Chenyan Zhao [1], Anna Chirkova[2], Staffan Rosenborg[3], Rodrigo Palma Villar[4], Johan Lindberg[4], Sven N. Hobbie [5]† and Lena E. Friberg [1]*†

[1]*Department of Pharmacy, Uppsala University, SE-75123, Uppsala, Sweden;* [2]*Juvabis AG, CH-8001, Zurich, Switzerland;* [3]*Department of Laboratory Medicine, Division of Clinical Pharmacology, Karolinska Institutet, Karolinska University Hospital, Huddinge, SE-14186, Stockholm, Sweden;* [4]*Department Chemical and Pharmaceutical Safety, RISE Research Institutes of Sweden, Sweden;* [5]*Institute of Medical Microbiology, University of Zurich, CH-8006, Zurich, Switzerland*

*Corresponding author. E-mail: lena.friberg@farmaci.uu.se
†Shared senior authorship.

Received 16 November 2021; accepted 15 June 2022

Background: Apramycin is under development for human use as EBL-1003, a crystalline free base of apramycin, in face of increasing incidence of multidrug-resistant bacteria. Both toxicity and cross-resistance, commonly seen for other aminoglycosides, appear relatively low owing to its distinct chemical structure.

Objectives: To perform a population pharmacokinetic (PPK) analysis and predict an efficacious dose based on data from a first-in-human Phase I trial.

Methods: The drug was administered intravenously over 30 min in five ascending-dose groups ranging from 0.3 to 30 mg/kg. Plasma and urine samples were collected from 30 healthy volunteers. PPK model development was performed stepwise and the final model was used for PTA analysis.

Results: A mammillary four-compartment PPK model, with linear elimination and a renal fractional excretion of 90%, described the data. Apramycin clearance was proportional to the absolute estimated glomerular filtration rate (eGFR). All fixed effect parameters were allometrically scaled to total body weight (TBW). Clearance and steady-state volume of distribution were estimated to 5.5 L/h and 16 L, respectively, for a typical individual with absolute eGFR of 124 mL/min and TBW of 70 kg. PTA analyses demonstrated that the anticipated efficacious dose (30 mg/kg daily, 30 min intravenous infusion) reaches a probability of 96.4% for a free AUC/MIC target of 40, given an MIC of 8 mg/L, in a virtual Phase II patient population with an absolute eGFR extrapolated to 80 mL/min.

Conclusions: The results support further Phase II clinical trials with apramycin at an anticipated efficacious dose of 30 mg/kg once daily.

Introduction

Apramycin is an aminoglycoside that has been used in veterinary infectious disease since the 1980s but is not available for human use. In face of the unmet clinical need for new antibacterial agents against MDR bacteria, EBL-1003, a crystalline free base of apramycin, has been developed in collaboration with the European Gram-Negative Antibacterial Engine (ENABLE)[1] project.

Apramycin possesses a unique chemical structure distinct from other aminoglycosides and of lower toxicity.[2–4] The distinct structure also confers apramycin a broad spectrum of antibacterial activity and minimal cross-resistance. Numerous *in vitro* and *in vivo* studies have demonstrated robust apramycin activity and efficacy against highly drug-resistant Gram-negative clinical isolates, including *Acinetobacter baumannii* (*A. baumannii*), *Pseudomonas aeruginosa* (*P. aeruginosa*), and Enterobacterales[5–11] as well as Gram-positive bacteria and mycobacteria.[12–14] This emerging evidence has supported the compound to move forward in the development pipeline to a Phase I first-in-human randomized clinical trial (ClinicalTrials.gov Identifier: NCT04105205).

The Phase I trial was designed to assess the safety, tolerability, and pharmacokinetics (PK) in healthy volunteers and expected to form the basis for developing the compound for intravenous use in patients with relevant systemic Gram-negative infections. A secondary objective of the trial was to perform a population PK

Table 1. Summary of demographics, vital signs and laboratory measurements of the 30 volunteers receiving apramycin

Continuous parameters	Min.	Q1	Median	Mean	Q3	Max.
Age (years)	18.0	24.8	32.5	31.5	37.0	45.0
BMI (kg/m^2)	18.6	22.4	23.9	23.9	25.5	29.6
TBW (kg)	60.4	66.2	72.8	73.7	81.6	87.4
Height (cm)	157	172	179	177	182	189
Cys-C (mg/L)	0.69	0.80	0.87	0.89	0.98	1.10
KIM-1 (μg/L)	0.01	0.15	0.25	0.39	0.60	1.83
Scr (mg/dL)	0.56	0.81	0.85	0.86	0.93	1.03
eGFR (mL/min/1.73 m^2)	93.0	107	114	113	121	137
BUN (mg/dL)	7.00	11.0	12.0	12.1	13.0	16.0
BSA (m^2)	1.71	1.79	1.90	1.90	1.99	2.13
Absolute eGFR (mL/min)	91.9	117	124	124	132	157
Categorical parameters	**Count**					
Sex						
Male	28					
Female	2					
Race						
Black or African American	1					
White	29					
Ethnicity						
Not Hispanic or Latino	30					

Absolute eGFR=eGFR × BSA/1.73; BSA, body surface area, $=\sqrt{TBW*Height/3600}$; BMI, body mass index; BUN, blood urea nitrogen; Cys-C, serum cystatin C; eGFR, glomerular filtration rate estimated using CKD-EPI equation; KIM-1, kidney injury molecule 1 (not normalized to urine creatinine); Q1, first quartile; Q3, third quartile; Scr, serum creatinine; TBW, total body weight.

(PPK) analysis based on apramycin concentrations collected in plasma and urine. In PPK models, both the typical trends and the variability are characterized, and covariate relationships can be quantified. Such models are therefore of value for simulating PTA in a population to support dose regimen selection in the development of new antimicrobial agents.[15] Allometric scaling of apramycin PK parameters from four preclinical species has resulted in predicted human parameters and concentration–time profiles that were similar to those of gentamicin, thus highlighting its PK similarity to other aminoglycosides.[16] Aminoglycosides are clinically administered in mg per kg with dosing adjustments in case of impaired renal function. Renal elimination has also been demonstrated to be the dominating elimination pathway for apramycin in preclinical studies.[4] Therefore, estimated glomerular filtration rate (eGFR) can be expected to be an important covariate for dosing adjustment in various groups of patients also for apramycin.

Pre-clinical studies have confirmed that for apramycin, as other aminoglycosides, the AUC of the unbound drug to MIC ratio (*f*AUC/MIC) is a pharmacokinetic–pharmacodynamic (PKPD) index correlated with bacterial response.[9,16] In a murine thigh infection model of four *Escherichia coli* (*E. coli*) strains, targets have been suggested to be plasma *f*AUC/MIC of 34.5 and 76.2 for stasis and 1 $\log_{10}$ kill, respectively.[16] In a murine lung model infected by an *A. baumannii* strain, the epithelial lining fluid (ELF) *f*AUC/MICs of 6.31, 7.26 and 8.34 for stasis, 1 $\log_{10}$ and 2 $\log_{10}$ kill, respectively, have been predicted from plasma *f*AUC/MIC using a lung penetration ratio of 0.88.[9] Based on these findings, a human efficacious dose of 30 mg/kg once daily has been suggested.[9,16] This dose regimen was also recently predicted to be efficacious in clinical pneumonia caused by Gram-negative bacteria based on translational *in vitro* and *in vivo* PKPD modelling.[17]

Herein, we describe the PPK model development based on both plasma and urine concentration measurements from the first-in-human study. The PPK model was subsequently applied to perform PTA analyses to explore the anticipated human efficacious dose in patients for Phase II clinical studies of apramycin.

Patients and methods

Study design and protocol

The EBL-1003 (apramycin) Phase I study JUV18-01 in healthy volunteers was a double-blind, randomized, placebo-controlled, single ascending dose trial. This trial was conducted in compliance with International Council for Harmonization E6 (R2) Good Clinical Practice provisions, applicable regulatory and legal requirements (EudraCT number 2019-000246-35 and ethical approval AM-2019-015 PB-0159 Ethik-Kommision, Landesärztekammer Baden-Württemberg), and the principles of the Declaration of Helsinki. Written informed consent was obtained from all subjects prior to participation in the trial.

Healthy males or females (of non-childbearing potential) aged 18–45 years (inclusive) were eligible for the study. Those with certain prior or concomitant illnesses, medications and procedures were excluded.

A total sample size of 40 subjects were enrolled in the trial and consecutively grouped into five sequential dose cohorts, i.e. 0.3, 1.2, 3.6, 10.8 and 30 mg/kg. In each cohort, there were eight individuals including two placebo-controls. Apramycin was administered as a single dose in the unit of mg (rounded to one decimal place) calculated based on the subject's total body weight (TBW, rounded to one decimal place) and infused intravenously (IV) over 30 min. For each subject, plasma samples

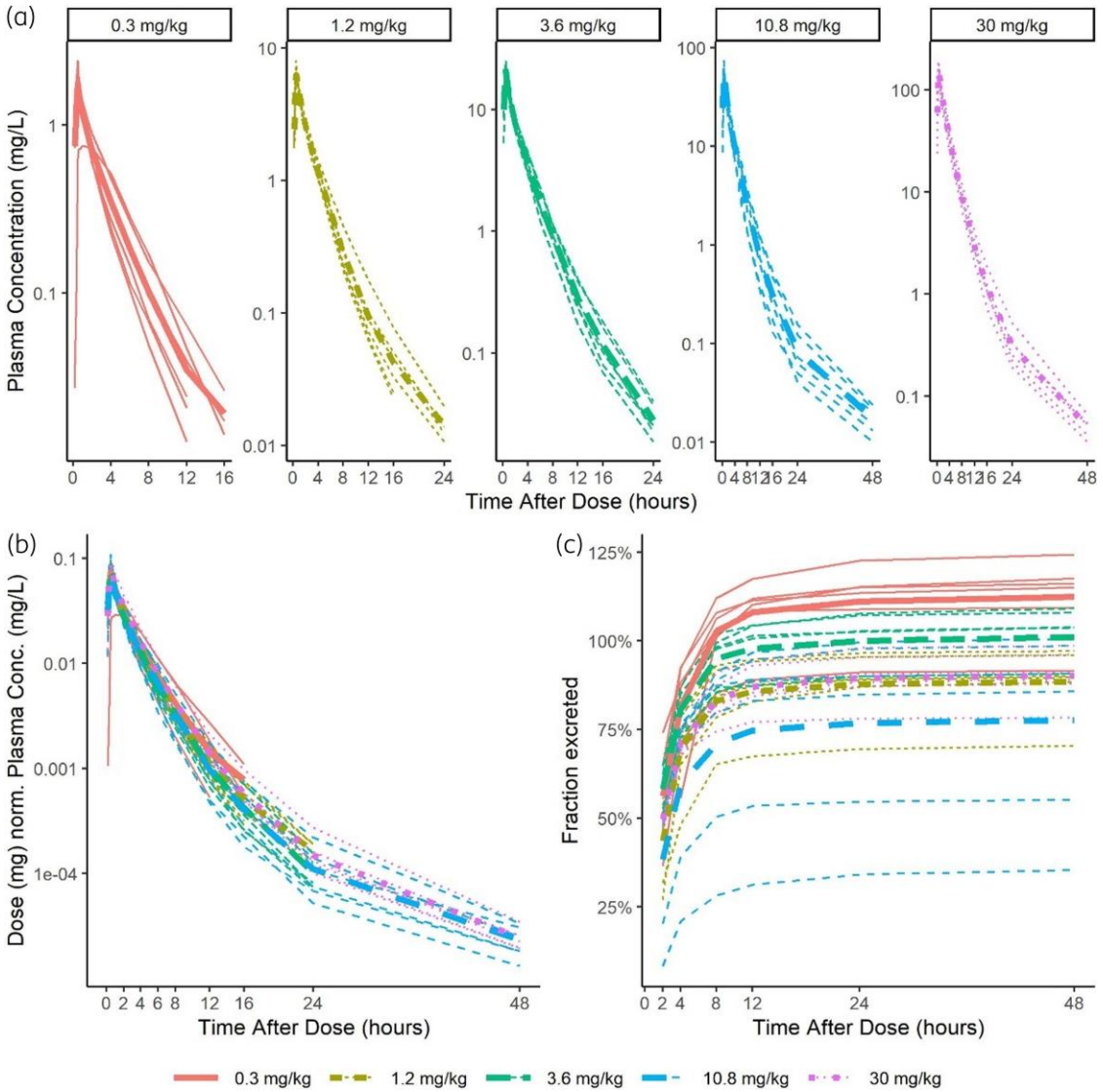

Figure 1. Apramycin (a) plasma concentrations stratified by dose cohort, (b) dose-normalized plasma concentrations and (c) accumulated fraction of administered drug amount excreted in urine over time profiles, coloured by respective dose cohort. Individual profiles are shown as thinner lines; group means are shown as thicker lines. Data below the limit of quantification are excluded or set to half of the limit in calculations for plasma or urine data, respectively.

were collected at 17 timepoints (0, 0.17, 0.33, 0.5, 0.58, 0.75, 1, 1.5, 2, 3, 4, 6, 8, 12, 16, 24 and 48 h after the start of the infusion) and urine samples were collected over each of the following intervals 0–2, 2–4, 4–8, 8–12, 12–24, and 24–48 h after the start of the infusion.

Various demographic characteristics, vital signs and laboratory measurements were recorded for each enrolled subject during screening, pre-dose/baseline, treatment period, and/or follow-up visits. In the scope of this PPK modelling and simulation study, the variables of interest as potential covariates were age, sex, race, ethnicity, height and BMI collected during screening as well as TBW, serum cystatin C (Cys-C), serum creatinine (Scr), blood urea nitrogen (BUN), and absolute urinary kidney injury molecule 1 (KIM-1) collected pre-dose. eGFR was calculated according to Chronic Kidney Disease Epidemiology Collaboration (CKD-EPI) equation to assess renal function (Eq. 1),

$$eGFR = 141 \times \min(Scr/\kappa, 1)^{\alpha} \times \max(Scr/\kappa, 1)^{-1.209} \times 0.993^{Age} \times 1.018\ [\text{if female}]\ \times 1.159\ [\text{if black}] \quad (1)$$

where eGFR is in mL/min/1.73 m^2, Scr is in mg/dL, age is in years, κ is 0.7 for females and 0.9 for males, α is −0.329 for females and −0.411 for males, min indicates the minimum of Scr/κ or 1, and max indicates the maximum of Scr/κ or 1. Body surface area (BSA) corrected eGFR, also known as absolute eGFR, was calculated using Eqs. 2 and 3,

$$BSA = \sqrt{\frac{TBW \times height}{3600}} \quad (2)$$

$$BSA\ corrected\ eGFR\ (absolute\ eGFR) = \frac{eGFR \times BSA}{1.73} \quad (3)$$

where BSA is in m^2, TBW is in kg, height is in cm, and absolute eGFR in mL/min.

Drug concentration analytical methods

The concentration of apramycin in human plasma and urine was reported in the unit of μmol/L and converted into mg/L in the PPK analysis using a

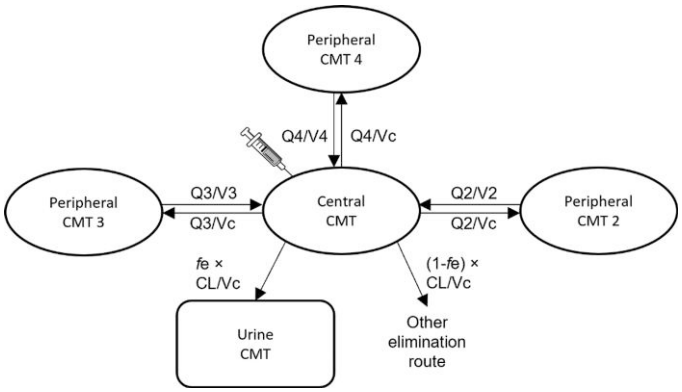

Figure 2. Schematic illustration of the developed apramycin population pharmacokinetic model. The central compartment (cmt), where drug is administered and plasma concentrations are observed, is connected reversibly to three parallel peripheral compartments (cmt 2–4). A large fraction of apramycin (*fe* %) is renally eliminated to the urine cmt while the rest is through other routes. Urine collections are from urine cmt. CL and Vc are clearance and volume of the central cmt, respectively. Q2, Q3, and Q4 are intercompartmental clearances between central cmt and cmt 2, 3, and 4, respectively. V2, V3, and V4 are volumes of cmt 2, 3, and 4, respectively.

molecular weight of 539.58 g/mol. The concentration was determined following protein precipitation with 30% trichloroacetic acid, using LC-MS/MS with kanamycin as an internal standard. Chromatographic separation was performed on a Waters XSelect HSS T3 column (2.5 μm, 2.1×150 mm) at 40°C. The mobile phase consisted of 0.1% formic acid in Milli-Q water (MPA) and 0.1% formic acid in 65% acetonitrile, 30% methanol and 5% isopropanol (MPB). A gradient at a flow rate of 0.3 mL/min MPB was run: 0–0.5 min 10%, 0.5–2.5 min 10%–95%; 2.5–3.4 min 95%; 3.4–3.5 min 95%–10%; 3.5–5.0 min 10%. The methods were validated according to the EMA guideline on bioanalytical method validation.[18] The lower and upper limits of quantification (LOQ) were 0.02 and 16.0 μmol/L (0.011 and 8.6 mg/L), 0.2 and 160 μmol/L (0.11 and 86 mg/L) for plasma and urine samples, respectively. Samples with concentrations above the upper LOQ were diluted with human plasma or urine before analysis. Blank matrices used for sample dilution were obtained from a commercial vendor (Novakemi AB) for human plasma and from healthy volunteer donors for human urine. The matrices were stored at −20°C prior to use. Calibration standards and quality control (QC) samples were prepared in blank human plasma or urine. Inter-run accuracy of QC samples ranged between 93.7% and 98.4%. Inter-run precision (coefficient of variation) was 2.0% to 5.8%.

Population PK analysis

Software, data set, and model selection and assessment criteria

The PPK analysis was performed in the nonlinear mixed-effects modelling software NONMEM® version 7.4.4 (ICON Development Solutions, San Antonio, TX),[19] with the auxiliary software PsN (https://uupharmacometrics.github.io/PsN/) version 5.0.[20] The R software environment (https://www.r-project.org/) version 4.0.2 embedded in RStudio was used for statistical computing and plotting graphics. Loaded R packages included *Xpose4* version 4.7.0[20] for model diagnostic plots and mrgsolve 0.10.4[21] for illustrating the impact of covariates and for PTA simulations.

Samples below lower LOQ (BLQ) were handled using the likelihood-based M3 method.[22] Model estimation method was the conditional Laplace with interaction. The *Log-transformation both sides* approach was implemented by converting both observed and predicted apramycin concentrations to ln-scale.

NONMEM output objective function value (OFV), which is asymptotically χ^2 distributed, was used to evaluate statistical significance for inclusion of additional parameters. For nested models, a change in OFV (*d*OFV) ≥3.84 with one parameter difference [i.e. $P<0.05$, 1 degree of freedom (*df*)] was considered statistically significant.

Developed models were evaluated by prediction-based diagnostic plots (with consideration of shrinkage), simulation-based visual predictive checks (VPCs; $n=500$) as well as scientific plausibility and parameter precision. The latter was derived by a non-parametric dose cohort-stratified bootstrap ($n=2000$).

Population PK model development with plasma data

The model development process was stepwise. First, a model was built using only plasma data. Compartmental models with linear or non-linear Michaelis-Menten elimination were explored. Inter-individual variability (IIV, log-normally distributed) and residual error (RUV, proportional in normal scale) models were investigated.

Covariates were tested for significance to explain IIV. Since aminoglycosides are known to mainly be eliminated through renal excretion, eGFR on clearance (CL), expressed as in Eq. 4, was the first evaluated relationship.

$$CL = \theta_1 + \left(\frac{eGFR}{Median\ eGFR}\right) \times \theta_2 \quad (4)$$

where θ_1 and θ_2 represent estimated non-renal clearance and renal clearance, respectively. TBW was then tested allometrically on all fixed effect PK parameters with exponents being fixed to 0.75 for clearance parameters, and 1 for volume parameters.[23] This was followed by the test of age on all parameters using a power model (Eq. 5).

$$CL = \theta_1 \times \left(\frac{Age}{Median\ Age}\right)^{\theta_2} \quad (5)$$

where θ_1 is the typical CL value for a subject with a median age and θ_2 is the estimated exponent. Other covariates of interest, Cys-C, Scr, BUN, and KIM-1 were tested using a power model as well by the PsN stepwise covariate model (SCM) tool. *P* values set for a forward inclusion step and a backward elimination step were 0.05 and 0.001 for 1 *df*, respectively. Sex, race, or ethnicity were not tested given their unbalanced distribution in the data set.

To meet the recommendation in the guidelines[24,25] to use an absolute measure of renal function (in mL/min) in the dosing recommendations for patients with reduced renal function, the fit of absolute eGFR was explored to replace eGFR with or without TBW.

Population PK model development with urine data

Once the model building for the plasma data was considered final, urine data was incorporated to determine the portion of drug being renally cleared. The model structure and parameters estimated from the plasma data were first fixed. A urine compartment was introduced to which apramycin was excreted and the compartment was emptied at the end of each sample collection interval. The estimated renal fractional excretion (*fe*) was defined as the percentage of eliminated apramycin that goes to the urine compartment (Eq. 6),

$$\frac{dA_{Urine}}{dt} = \frac{CL}{Vc} \times A_{Central} \times fe \quad (6)$$

where A_{Urine} and $A_{Central}$ represent drug amount in the urine and central compartment, respectively. CL and Vc are the clearance and volume of

Table 2. Parameter estimates and bootstrap results of the final PPK models based on plasma data alone and on both plasma and urine data

Parameter	Unit	Description	Plasma data Mode (RSE) [2.5th–97.5th percentile][b]	Plasma + urine data Mode (RSE) [2.5th–97.5th percentile][b]
Fixed effect parameters				
CL[a]	L/h	CL from the central cmt	5.55 (2.45%) [5.29–5.83]	5.54 (2.38%) [5.29–5.82]
Vc	L	V of the central cmt	8.61 (5.48%) [7.73–9.66]	8.61 (5.27%) [7.75–9.66]
Q2	L/h	Q between central cmt and peripheral cmt 2	0.121 (7.83%) [0.10–0.14]	0.127 (7.29%) [0.11–0.15]
V2	L	V of the peripheral cmt 2	2.24 (3.85%) [2.11–2.43]	2.29 (3.58%) [2.16–2.48]
Q3	L/h	Q between central cmt and peripheral cmt 3	13.6 (7.68%) [11.1–15.5]	13.6 (7.34%) [11.5–15.6]
V3	L	V of the peripheral cmt 3	2.87 (14.3%) [2.14–3.87]	2.81 (13.2%) [2.05–3.66]
Q4	L/h	Q between central cmt and peripheral cmt 4	1.03 (14.5%) [0.70–1.34]	1.01 (13.4%) [0.73–1.33]
V4	L	V of the peripheral cmt 4	2.44 (6.25%) [2.10–2.74]	2.38 (5.71%) [2.10–2.67]
Fe	–	Fraction of eliminated drug from central to urine cmt	–	0.900 (2.65%) [0.85–0.94]
Inter-individual variability (IIV)[c]				
CL	%	IIV in CL (CV)	14.4 (10.2%) [11.4–17.4]	14.4 (10.0%) [11.5–17.4]
Vc	%	IIV in Vc (CV)	32.6 (17.5%) [22.9–46.7]	33.1 (19.8%) [24.0–50.5]
V3	%	IIV in V3 (CV)	55.8 (36.7%) [20.7–107]	61.2 (41.9%) [35.1–132]
V4	%	IIV in V4 (CV)	13.9 (15.9%) [9.1–18.5]	13.9 (15.0%) [9.33–18.6]
RUV plasma	%	IIV in RUV (CV)	69.3 (26.7%) [27.9–104]	69.5 (22.9%) [33.1–102]
RUV urine	%	IIV in RUV (CV)	–	38.5 (24.5%) [19.8–62.9]
CL∼Vc[d]	–	Correlation between IIV of CL and Vc	0.52 (25.0%) [0.25–0.76]	0.52 (27.4%) [0.17–0.95]
CL∼V3[d]	–	Correlation between IIV of CL and V3	−0.40 (−39.5%) [−0.69 to −0.07]	−0.40 (−41.0%) [−0.69 to −0.02]
Vc∼V3[d]	–	Correlation between IIV of Vc and V3	−0.91 (−4.52%) [−0.98 to −0.81]	−0.92 (−4.03%) [−0.98 to −0.83]
Residual variability (RUV)[c]				
Prop plasma	%	Proportional RUV model for plasma data	8.51 (10.1%) [7.10–10.8]	8.79 (8.96%) [7.43–10.8]
Prop urine	%	Proportional RUV model for urine data	–	35.1 (8.02%) [29.3–40.9]

CL, clearance; CV, coefficient of variation, calculated by $\sqrt{\exp^{OMEGA}-1}$; Q, intercompartmental clearance; V, volume; and cmt, compartment.
[a]Typical CL normalized to an individual with absolute eGFR 124 mL/min and TBW 70 kg, following the equation CL = 5.55 (or 5.54) × (absolute eGFR/124) × (TBW/70)$^{0.75}$, where absolute eGFR is glomerular filtration rate estimated using CKD-EPI equation corrected by body surface area and TBW is total body weight.
[b]Mode is the reported parameter typical value from population pharmacokinetic models; relative standard error (RSE) and percentiles are from bootstrap (n = 2000). For the plasma + urine model, failed bootstrap samples (n = 4) were excluded from calculation.
[c]ETA shrinkages were 13% for V4 for both models, 22% for urine RUV for plasma + urine model, and 0% for others. Epsilon shrinkage was 1% and 2% for plasma model and plasma + urine model, respectively.
[d]$Correlation(A, B) = \frac{Covariance(A,\ B)}{\sqrt{OMEGA(A)\times OMEGA(B)}}$, where A and B are the two correlated IIVs.

central compartment, respectively, with covariates and IIV estimated from plasma data included. IIV in *fe* was tested. RUV for urine data was estimated separately.

The final model refinement step was conducted by re-estimating all parameters simultaneously using plasma and urine data. The significance of non-renal or non-linear clearance was re-evaluated to check if urine data would provide related information.

Relationships between covariates and PK profiles

A graphical description of covariates versus PK parameters of interest, i.e. concentration at 24 h after dose (C_{24h}) and AUC from 0 to 24 h after dose (AUC_{0-24}), and concentration–time curves were derived using the final plasma PPK model.

Pharmacodynamic (PD) target attainment simulation

In the PTA simulations, the final plasma PPK model (with RUV excluded) was used in combination with *f*AUC/MIC targets. Individual AUCs were calculated as the ratio of absolute administered dose and simulated individual CL. The unbound fraction (f_u) in human plasma has been determined to be 91.5% (details on plasma protein binding are presented in Figure S1, together with additional methods, available as Supplementary data at *JAC* Online). Selected target *f*AUC/MICs were 15, 30, 40, 60 and 90. Evaluated MICs ranged from 2 to 64 mg/L (2-fold increases) with MIC_{90} of 8 mg/L for Enterobacterales. The explored dose range was 20–40 mg/kg/day (increments of 5) and a TBW of 75 kg was adopted. Simulations were also conducted for patient populations, i.e. extrapolated from the healthy volunteer population, as suggested in the EMA guideline.[15] Absolute eGFRs were set to 80 mL/min (extrapolated, assuming same parameter-covariate relationship as in the final model) and 120 mL/min (interpolated) mimicking a patient population with mildly decreased renal function (as observed in patient population of Phase II for plazomicin)[26] or normal renal function, respectively. For the former population, CL IIV was inflated to 30% in line with the reported values in patients for aminoglycosides from USCAST[27–30] and to 60% to

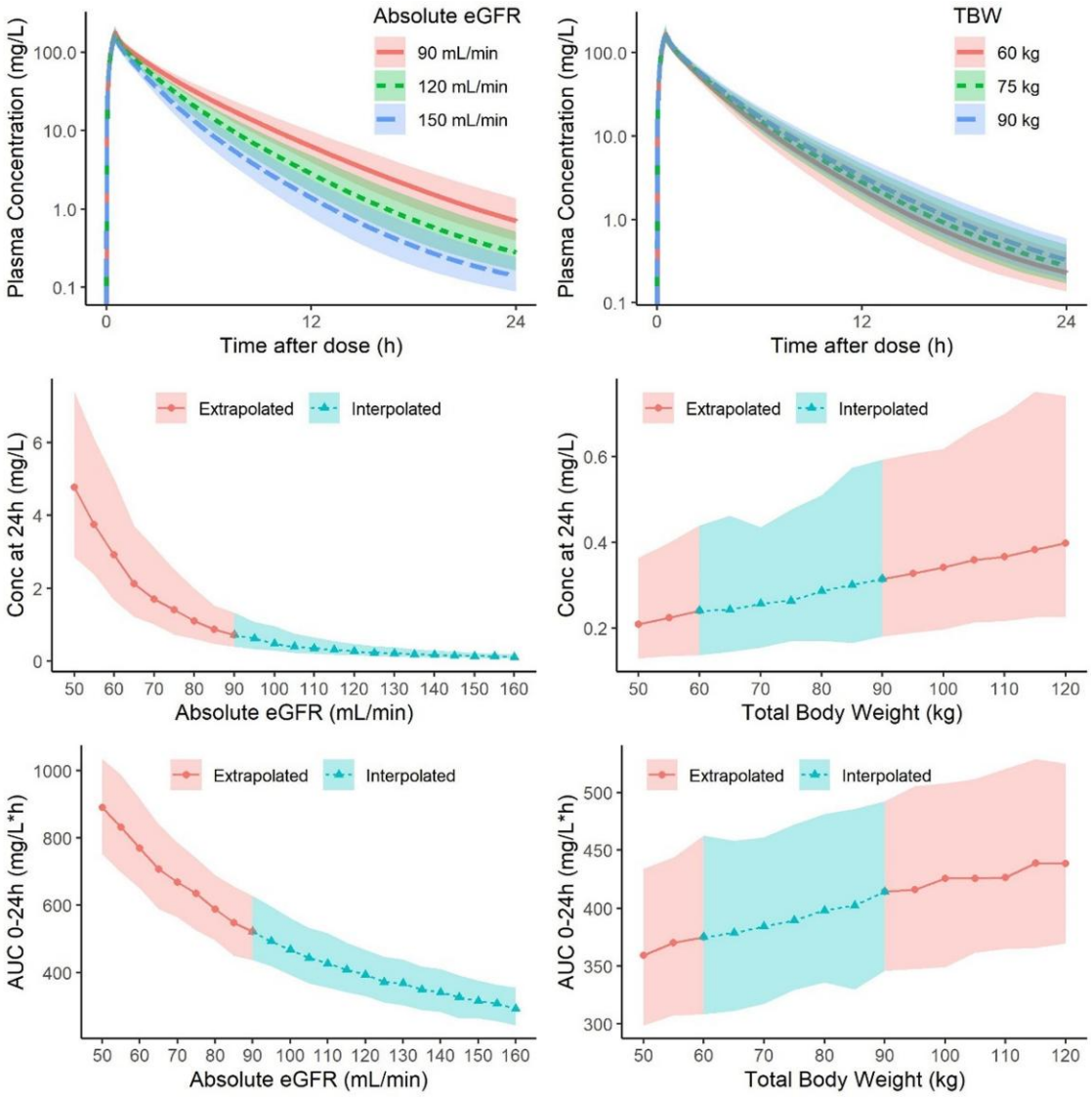

Figure 3. Relationships of the change in absolute eGFR (left column, absolute eGFR range 50–160 mL/min, increments of 5, when TBW set to 75 kg) and TBW (right column, WT range 50–120 kg, increments of 5, when absolute eGFR set to 120 mL/min) versus the change in concentration–time profiles (first row), concentration at 24 h after dose (second row) and AUC in the first 24 h after dose (third row), following a dose of 30 mg/kg administered intravenously over 30 min. The solid line is the median and the corresponding-coloured area is 80% prediction interval, based on 500 simulated individuals in each scenario. The colours and shapes indicate whether the range of covariate values were interpolated from the observed range in the first-in-human study, or extrapolated.

acknowledge a possible even larger IIV in some patient populations.[31] Parameter uncertainty was taken into account in the simulations, in line with FDA guidance,[32] by using samples from a bootstrap ($n=2000$) from the final model. For each sample and scenario, 1000 individuals were simulated.

Results

Subjects and observations

The 30 subjects who received EBL-1003 were analysed. Selected demographics, vital signs and laboratory measurements are summarized in Table 1. No obvious dose-related difference was observed between dose cohorts (Figure S2). There was no significant change in KIM-1 over time (data not shown). They contributed 480 plasma observations (with pre-dose samples excluded) and 179 urinary observations. Each apramycin concentration in urine was associated with a urine volume. One individual failed to produce any urine within the collection period 0–2 h post-dose. Thus, the collection time interval of the nominal 2–4 h sample was recorded as 0–4 h. One urine collection time was missing thus the nominal one was used. There was otherwise no missing data. There were 29 (6.0%) and 4 (2.2%) samples with concentrations BLQ for plasma and urine, respectively. Two BLQ plasma samples were reported as exact values

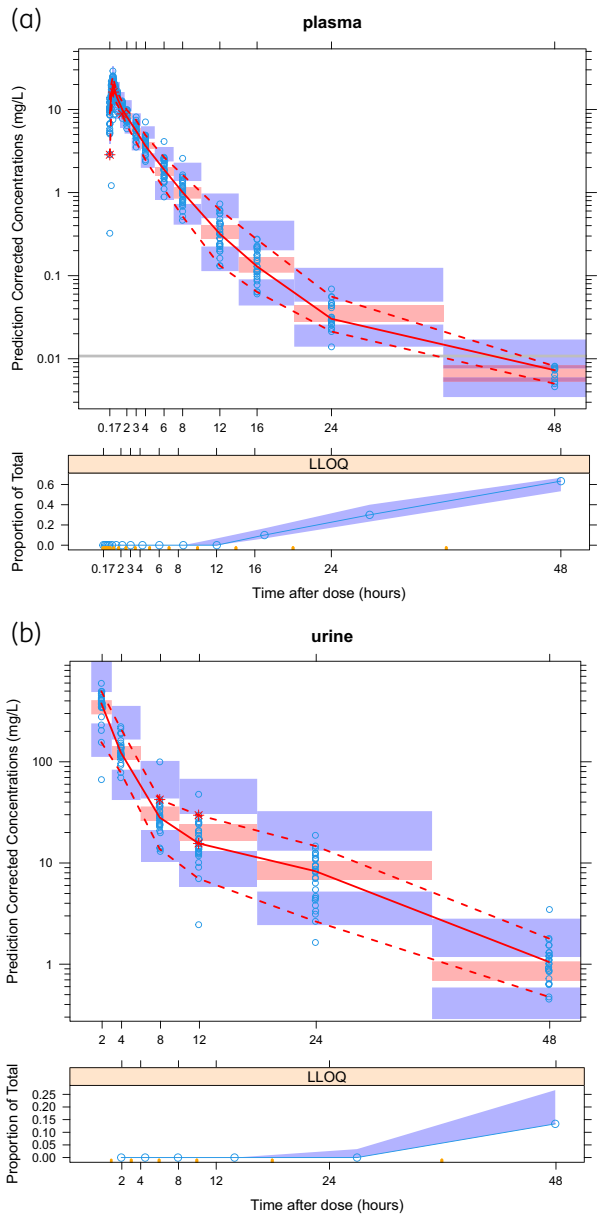

Figure 4. Prediction corrected visual predictive check (pcVPC) of the final population pharmacokinetic model developed from combined plasma and urine data for (a) plasma and (b) urine concentrations. In each subplot, the upper panel shows the fit of the observations above the limit of quantification (LOQ) with LOQ indicated by the grey line; observations are displayed as blue dots; red lines are the observed 5th, 50th, and 95th percentiles, blue and red fields are the corresponding 95% CI defined by simulations from the model. Red stars highlight where the observed percentile is outside the 95% CI. The lower panels show the fit of the observed proportion of the data below LOQ. The observed proportions are displayed as blue dots and blue fields are the corresponding 95% CI. For urine, time of observations are the end of the collection interval. A zoom-in plot providing greater resolution for the first 5 h of panel (a) plasma can be found in Figure S6. This figure appears in colour in the online version of *JAC* and in black and white in the print version of *JAC*.

(0.0198 and 0.0188 μmol/L, corresponding to 0.0107 and 0.0101 mg/L) and the reported values were kept in the dataset.

Dose-normalized plasma concentration–time profiles indicated no apparent deviation from dose linearity as the lines from all dose cohorts overlapped (Figure 1b). One individual in the lowest dose group (0.3 mg/kg) had a deviating profile during the first 1.5 h with 20%–97% lower concentrations compared with the mean of other subjects in the same dose group and timepoints. This subject was however kept in the analysis since absolute conditional weighted residuals were <5 and there was low impact on the final parameter estimates.

The observed accumulated fraction of dose excreted from urine over time is shown in Figure 1(c). There appeared to be some cohort (batch-assay) dependence in *fe*: the profiles had similar patterns among individuals in the same dose cohort. There was however no trend between *fe* and dose level. The observed *fe* varied across dose levels (group means range 77.7% to 112% until 48 h), with values over 100% reflecting variation and/or error in sample collection and measurement.

Developed PPK models

The final plasma PPK model was a mammillary four-compartment model where the central compartment is connected reversibly to three parallel peripheral ones (Figure 2, Table 2). The linear elimination was from the central compartment. A three-compartment model had a worse fit (*d*OFV >100, $df = 3$). Nonlinear CL did not perform better and there was no sign of a dose-dependent CL. IIVs were included in CL, Vc, V_3, and V_4, where V_3 and V_4 are the volumes of the third and fourth compartments, respectively. Covariances between IIVs in CL, Vc and V_3 were kept. IIV in RUV improved the model fit significantly (>450 OFV units).

eGFR on CL according to Eq. 4 resulted in five units drop of OFV. When the non-renal part was excluded, the fit was not worsened significantly (*d*OFV = 2, $df = 1$). When TBW was allometrically added to all clearance and volume parameters of the four compartments ($n = 8$), OFV reduced 43 units. Absolute eGFR resulted in a 10 unit lower OFV compared with eGFR, and addition of allometrically scaled TBW reduced OFV an additional 4 units. No other covariate relationships on top of absolute eGFR and TBW were identified.

The values reported in Table 2 represent a typical individual with absolute eGFR of 124 mL/min and TBW 70 kg. For a 30 mg/kg dose infused IV over 30 min, the typical derived values of AUC 0–infinity (AUC_{inf}, i.e. steady-state AUC), maximum concentration (C_{max}), C_{24h} and concentration at 48 hours (C_{48h}) were 378 mg·h/L, 170 mg/L, 0.217 mg/L and 0.0457 mg/L, respectively. An illustration of how absolute eGFR and TBW affect plasma PK profiles is shown in Figure 3.

The estimated *fe* was 90%, corresponding to an estimated renal clearance (CLr) of 4.99 L/h. Since filtration clearance (*fu**eGFR = 6.81 L/h, with eGFR = 124 mL/min) was higher than CLr, the data suggested apramycin reabsorption to be higher than tubular secretion. IIV in *fe* was excluded with no statistical worsening of the fit, while IIV in RUV for urine data was included (>20 *d*OFV). The urine data confirmed that non-renal or nonlinear clearance was not significant for apramycin. The parameter values from the final model based on combined plasma and urine data deviated only slightly from those based on plasma data alone (≤10% except for 15% for IIV in V_3, Table 2).

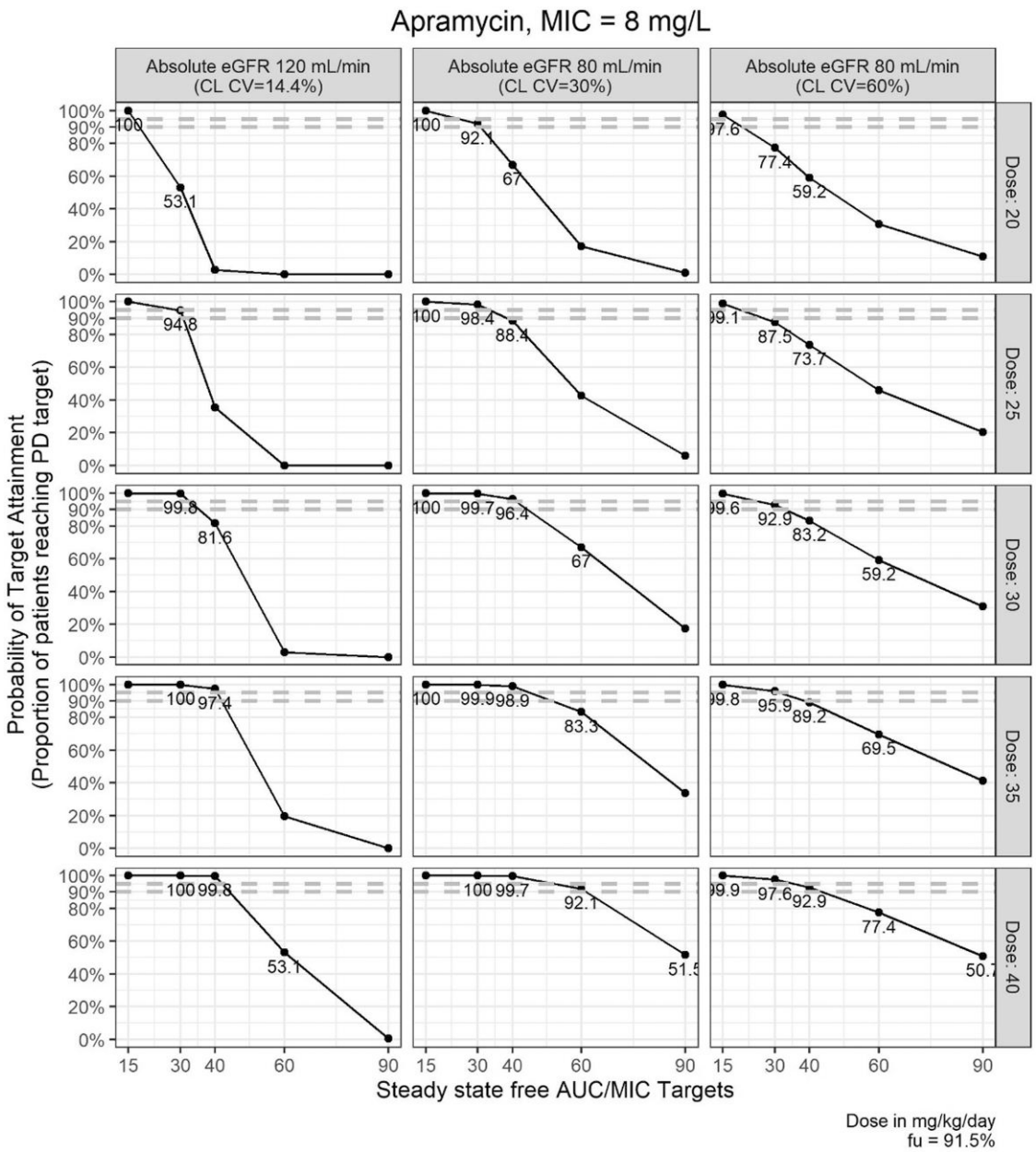

Figure 5. Apramycin PTA versus steady-state free AUC/MIC targets for an MIC of 8 mg/L under different daily doses in patients with TBW 75 kg and different renal function, based on 1000 simulated individuals in each scenario. Inter-individual variability (IIV) on clearance (CL) was set to coefficient of variation (CV) 14.4% for the interpolated and 30% or 60% for the extrapolated virtual patient population. Grey dashed lines indicate 90% and 95% PTA for reference. PTAs >50% and <100% are annotated. Individual AUCs were calculated as the ratio of absolute administered dose over model simulated individual CL. Absolute eGFR, estimated glomerular filtration rate (CKD-EPI equation) corrected by body surface area; TBW, total body weight. To note, some of the PTAs in the patient population were predicted to be lower than the corresponding PTAs in the population with normal renal function due to the larger IIV assumed in the former population.

Model evaluation

Model evaluations displayed here are based on the final model developed with both plasma and urine data. When the PK model was estimated on only plasma data the fit was similar. Both eta- and epsilon-shrinkage were <25% (Table 2). The bootstrap resulted in RSEs <30%, except for the ones related to V3 IIVs, which were around 40% (Table 2).

The prediction-based goodness-of-fit plots (Figures S3 to S5) indicate that for plasma concentrations, the final model can fit the observations reasonably well considering that some data were BLQ. There was a trend of over-prediction at high urine concentrations, likely due to the relatively sparse sampling and larger experimental variability in the urine data. VPCs for the final model, as illustrated in Figure 4 (prediction-corrected, zoom-in plot

shown in Figure S6) and Figure S7 (stratified on dose cohorts) illustrate good simulation properties.

Simulated PTA

PTA simulation plots are shown in Figure S8 and summarized in Table S1. The numeric summary for an MIC of 8 mg/L is illustrated in Figure 5. Figure S9 shows the median and 90% and 95% CIs of achievable *f*AUC/MIC in the simulated populations treated with 30 mg/kg/day. A 30 mg/kg/day dose (IV over 30 min) showed PTAs of 100%, 99.7% and 96.4% with *f*AUC/MIC targets of 15, 30 and 40, respectively, in an assumed patient population with mild renal impairment (absolute eGFR 80 mL/min and 30% IIV in CL). The PTA was <90% in the other two evaluated populations for an *f*AUC/MIC target of 40. For a dose of 30 mg/kg once daily, a PTA of over 90% was predicted for targets of 60 and 90 and MICs of ≤4 mg/L and ≤2 mg/L, respectively.

Discussion

A four-compartment linear PPK model adequately described apramycin disposition using plasma and urine concentrations collected over a 48 h period after the start of infusion from 30 randomized volunteers. The absolute eGFR was proportional to CL and TBW allometrically scaled all fixed effect parameters. Most of the administered drug (estimated *fe* = 90%) was excreted renally. Simulations from the final PPK model suggested that a 30 mg/kg dose would result in at least 95% PTA for an MIC of 8 mg/L using *f*AUC/MIC targets ≤40 in a well-controlled virtual patient population with mildly reduced renal function, representing a possible target population in subsequent Phase II clinical trials. Moreover, all dose levels, including the 30 mg/kg dose, were safe and well tolerated with no medically relevant effects on renal or ontological function parameters (data not shown).

The rich sampling design allowed for a four-compartment model to describe the disposition of apramycin. The PPK of other aminoglycosides has frequently been described by multi-compartment models when the PK sampling has so allowed.[26,33,34] The estimated parameter values and included covariates also showed similar PK properties for apramycin as for other aminoglycosides.[35] For example, the estimated CL of 5.5 L/h (0.0786 L/h/kg) was similar to the reported values of other aminoglycosides (4.75–7.32 L),[26–29,36] when normalized to creatinine clearance 124 mL/min and TBW 70 kg. Moreover, the predicted CL in healthy humans using allometric scaling from animal PK parameters was 7.07 L/h.[16]

The estimated steady-state volume of distribution (V_{dss}) of 16 L (0.23 L/kg) is similar to other aminoglycosides (13–20 L)[31,36,37] in healthy volunteers. However, V_{dss} has been reported to be higher in patients (27–57 L).[26–29] This may be due to the PK variations caused by underlying pathophysiological conditions given that aminoglycosides are hydrophilic antimicrobials.[38] Differences in dosing regimens and sampling designs in these studies and the approximation used in calculation may also be reasons for differences in V_{dss}. Since AUC is not dependent on V_{dss} and antibacterial effect has correlated best to AUC/MIC,[9,16] there is no need to account for potential differences in V_{dss} between healthy volunteers and patients in PTA analysis.

Absolute eGFR reflects the kidneys' capacity to eliminate renally excreted drugs and given the estimated *fe* of 90%, renal function-based dosing of apramycin is warranted. In a study of plazomicin in patients, renal clearance was also found to be around 90% of the total.[26] As shown in Figure 3, a 30 mg/kg dose of apramycin may consequently result in AUC_{0-24} and C_{24h} (i.e. trough concentration) with increased risk for tolerability issues in individuals with absolute eGFR <60 mL/min. It may therefore be necessary to increase the dosing interval or reduce the administered dose in such patients with decreased renal function. Here, renal function is described by CKD-EPI-based eGFR, since CKD-EPI was used in apramycin Phase I safety evaluation and has been recommended for routine clinical use to estimate kidney function.[39]

In this study, we performed PTA analyses based on available healthy volunteer data. Moreover, the eGFR relationship identified in the PPK model was used to extrapolate, in additional PTA analyses, to an anticipated Phase II patient population with mildly reduced renal function (absolute eGFR = 80 mL/min[26]). This approach was part of the analysis plan and acknowledges that a purpose of this study is to inform dose selection for Phase II. This extrapolation strategy is also in line with the EMA guideline,[15] which suggests that if only healthy volunteer PK data are available, the PPK model should be adjusted so that the PTA simulation results reflect any changes in the PK covariates and PK parameters and the degree of IIV in the target patient population. Modelling and simulation are indeed a well-recognized tool for exploring dosing strategies under untested scenarios and for designing new studies.[40] It is however important to understand the underlying assumptions when extrapolating outside the studied conditions. Here, we make use of the eGFR relationship in healthy volunteers (absolute eGFR 91.9–157 mL/min) to extrapolate to an absolute eGFR of 80 mL/min, for a compound (and compound class) primarily eliminated by the kidneys. This could be regarded as an extrapolation with relatively high confidence. The variability in the PK parameters (CL IIV) is more uncertain and therefore illustrated for two scenarios (Figure 5). To note, we also included parameter uncertainty of the PK parameter estimates in the PTA analysis to further illustrate the uncertainties. In earlier stages of drug development, we made use of gentamicin PPK to predict the human efficacious dose since the PK of gentamicin and apramycin have been shown to be similar in preclinical studies.[9,16,17] This illustrates how model-informed drug development can be used to support drug development[41] before patient information is available. Defining the dose for Phase II based on a reduced eGFR also reduces the risk to suggest a dosing strategy that may lead to exposures above the studied range in Phase I and thereby increase the risk of toxicity.

The MIC range in the performed PTA analyses covered the reported MIC_{90} values for apramycin: 4 mg/L for *Klebsiella pneumoniae* and *Enterobacter* spp., 8 mg/L for *E. coli* and 16 mg/L for *A. baumannii*.[7] For *P. aeruginosa*, different MIC_{90} values have been reported for apramycin ranging from 8 mg/L (Table S1 in reference[42]) to 32 mg/L in a panel of highly aminoglycoside-resistant *P. aeruginosa* isolates with an MIC_{90} of >256 mg/L for both tobramycin and amikacin.[5] Provided that the EUCAST clinical breakpoint for amikacin is 16 mg/L, it may be conceivable to extrapolate a clinical breakpoint of 16 or 32 mg/L for apramycin as well. However, further studies with much larger panels of

P. aeruginosa clinical isolates and pharmaceutical-grade drug substance have yet to be conducted to determine robust and reliable epidemiological cutoff values.

The range of PTA targets were based on preclinical studies of apramycin as well as general targets for aminoglycosides. Considering the target ELF *f*AUC/MICs of 8 defined based on a 2 $\log_{10}$ kill of *A. baumannii* in a mouse pneumonia model,[9] apramycin has shown promise against respiratory tract infections. On the other hand, we acknowledge the lower PTAs at higher targets. For example a target *f*AUC/MIC of 76 (based on 1 $\log_{10}$ kill of *E. coli*) has been suggested for systemic infections based on PK/PD studies in the neutropenic thigh infection model.[16] This difference in target is in line with what has been identified for aminoglycosides against Enterobacteriaceae in non-clinical studies; targets are 2–20 times higher in the thigh compared with pneumonia infection models.[30] This difference may be because of a longer retention time of aminoglycosides in lung[43] and reduced penetration of polar aminoglycosides into thigh tissue, resulting in higher drug exposure and *f*AUC in lung than in thigh.

The collection of urine samples enabled a direct characterization of the fraction excreted renally. Although up to 3-fold (35% versus 124% at 48 h) between-subject variation was observed in urinary recovery ratio (Figure 1c), it was not significant to estimate IIV in *fe* in the model, which may indicate that the observed variability was explained by IIVs of other systemic distribution parameters (e.g. CL and Vc) in addition to the unexplained RUV. Further studies in patient populations will further quantify the importance of renal function and TBW in dosing adjustment.

To conclude, the developed apramycin PPK models successfully described the first-in-human Phase I plasma and urine concentrations. The PK properties were similar to other aminoglycosides and the analyses will support further studies in patients. The PTA analysis suggested a promising efficacy of the drug, covering MICs up to 8 mg/L for a 30 mg/kg dose and a target of 40. The extrapolation to a 'typical' patient population serves as a starting point for further clinical development, including Phase II trials, and needs to be verified.

Funding

Research leading to these results was conducted as part of the ND4BB European Gram-Negative Antibacterial Engine (ENABLE) Consortium (www.nd4bb-enable.eu) and has received funding from the Innovative Medicines Initiative Joint Undertaking under grant agreement no. 115583, resources of which are composed of financial contribution from the European Union's Seventh Framework Programme (FP7/2007-2013) and The European Federation of Pharmaceutical Industries and Associations (EFPIA) companies in-kind contribution. The ENABLE project is also financially supported by contributions from Academic and Small and medium-sized enterprise (SME) partners. C.Z. was also supported by the Swedish Research Council [grant no. 2018-03296 to L.E.F.].

Transparency declarations

A.C. is an employee and S.N.H. a co-founder of Juvabis AG, a startup biotech company with an interest in aminoglycoside therapeutics. S.R. was contracted through the Karolinska University Hospital as medical monitor, i.e. sponsor's medical representative, for the Phase I trial. All other authors: none to declare.

Supplementary data

Additional Methods, Table S1 and Figures S1 to S9 are available as Supplementary data at *JAC* Online.

References

1 Olliver M, Griestop L, Hughes D *et al.* ENABLE: an engine for European antibacterial drug discovery and development. *Nat Rev Drug Discov* 2021; **20**: 407–8. doi:10.1038/d41573-021-00074-y

2 Matt T, Ng CL, Lang K *et al.* Dissociation of antibacterial activity and aminoglycoside ototoxicity in the 4-monosubstituted 2-deoxystreptamine apramycin. *Proc Natl Acad Sci USA* 2012; **109**: 10984–9. doi:10.1073/pnas.1204073109

3 Ishikawa M, García-Mateo N, Čusak A *et al.* Lower ototoxicity and absence of hidden hearing loss point to gentamicin C1a and apramycin as promising antibiotics for clinical use. *Sci Rep* 2019; **9**: 2410. doi:10.1038/s41598-019-38634-3

4 Becker K, Cao S, Nilsson A *et al.* Antibacterial activity of apramycin at acidic pH warrants wide therapeutic window in the treatment of complicated urinary tract infections and acute pyelonephritis. *EBioMedicine* 2021; **73**: 103652. doi:10.1016/j.ebiom.2021.103652

5 Kang AD, Smith KP, Eliopoulos GM *et al. In vitro* apramycin activity against multidrug-resistant *Acinetobacter baumannii* and *Pseudomonas aeruginosa*. *Diagn Microbiol Infect Dis* 2017; **88**: 188–91. doi:10.1016/j.diagmicrobio.2017.03.006

6 Kang AD, Smith KP, Berg AH *et al.* Efficacy of apramycin against multidrug-resistant *Acinetobacter baumannii* in the murine neutropenic thigh model. *Antimicrob Agents Chemother* 2018; **62**: 188–91.

7 Juhas M, Widlake E, Teo J *et al. In vitro* activity of apramycin against multidrug-, carbapenem- and aminoglycoside-resistant Enterobacteriaceae and *Acinetobacter baumannii*. *J Antimicrob Chemother* 2019; **74**: 944–52. doi:10.1093/jac/dky546

8 Riedel S, Vijayakumar D, Berg G *et al.* Evaluation of apramycin against spectinomycin-resistant and -susceptible strains of *Neisseria gonorrhoeae*. *J Antimicrob Chemother* 2019; **74**: 1311–6. doi:10.1093/jac/dkz012

9 Becker K, Aranzana-Climent V, Cao S *et al.* Efficacy of EBL-1003 (apramycin) against *Acinetobacter baumannii* lung infections in mice. *Clin Microbiol Infect* 2021; **27**: 1315–21. doi:10.1016/j.cmi.2020.12.004

10 Hao M, Shi X, Lv J *et al. In vitro* activity of apramycin against carbapenem-resistant and hypervirulent *Klebsiella pneumoniae* isolates. *Front Microbiol* 2020; **11**: 425. doi:10.3389/fmicb.2020.00425

11 Nafplioti K, Galani I, Angelidis E *et al.* Dissemination of international clone II *Acinetobacter baumannii* strains coproducing OXA-23 carbapenemase and 16S rRNA methylase armA in Athens, Greece. *Microb Drug Resist* 2020; **26**: 9–13. doi:10.1089/mdr.2019.0075

12 Truelson KA, Brennan-Krohn T, Smith KP *et al.* Evaluation of apramycin activity against methicillin-resistant, methicillin-sensitive, and vancomycin-intermediate *Staphylococcus aureus* clinical isolates. *Diagn Microbiol Infect Dis* 2018; **92**: 168–71. doi:10.1016/j.diagmicrobio.2018.05.018

13 Selchow P, Ordway DJ, Verma D *et al.* Apramycin overcomes the inherent lack of antimicrobial bactericidal activity in *Mycobacterium abscessus*. *Antimicrob Agents Chemother* 2022; **66**: e0151021. doi:10.1128/aac.01510-21

14 Meyer M, Freihofer P, Scherman M *et al. In vivo* efficacy of apramycin in murine infection models. *Antimicrob Agents Chemother* 2014; **58**: 6938–41. doi:10.1128/AAC.03239-14

15 European Medicines Agency. Guideline on the use of pharmacokinetics and pharmacodynamics in the development of antimicrobial

medicinal products EMA/CHMP/594085/2015. 2015. https://www.ema.europa.eu/en/documents/scientific-guideline/guideline-use-pharmacokinetics-pharmacodynamics-development-antimicrobial-medicinal-products_en.pdf.

16 Sou T, Hansen J, Liepinsh E *et al*. Model-informed drug development for antimicrobials: translational PK and PK/PD modeling to predict an efficacious human dose for apramycin. *Clin Pharmacol Ther* 2021; **109**: 1063–73. doi:10.1002/cpt.2104

17 Aranzana-Climent V, Hughes D, Cao S *et al*. Translational *in vitro* and *in vivo* PKPD modelling for apramycin against Gram-negative lung pathogens to facilitate prediction of human efficacious dose in pneumonia. *Clin Microbiol Infect* 2022. doi: 10.1016/j.cmi.2022.05.003

18 European Medicines Agency. Guideline on bioanalytical method validation EMEA/CHMP/EWP/192217/2009. 2009. https://www.ema.europa.eu/en/documents/scientific-guideline/guideline-bioanalytical-method-validation_en.pdf.

19 Beal S, Sheiner L, Boeckmann A, Bauer R (eds). NONMEM 7.4 Users Guides (1989–2018). https://nonmem.iconplc.com/nonmem744/guides.

20 Keizer RJ, Karlsson MO, Hooker A. Modeling and simulation workbench for NONMEM: tutorial on Pirana, PsN, and Xpose. *CPT Pharmacometrics Syst Pharmacol* 2013; **2**: e50. doi:10.1038/psp.2013.24

21 Baron KT, Gastonguay MR. Simulation from ODE-based population PK/PD and systems pharmacology models in R with mrgsolve. 2015. https://metrumrg.com/wp-content/uploads/2017/06/Baron_ACOP_2015.10.pdf.

22 Beal SL. Ways to fit a PK model with some data below the quantification limit. *J Pharmacokinet Pharmacodyn* 2001; **28**: 481–504. doi:10.1023/A:1012299115260

23 Holford N. Pharmacokinetic variability due to environmental differences. *Transl Clin Pharmacol* 2017; **25**: 59–62. doi:10.12793/tcp.2017.25.2.59

24 Center for Drug Evaluation and Research. Pharmacokinetics in patients with impaired renal function—study design, data analysis, and impact on dosing and labeling FDA-2010-D-0133. 2020. https://www.fda.gov/regulatory-information/search-fda-guidance-documents/pharmacokinetics-patients-impaired-renal-function-study-design-data-analysis-and-impact-dosing-and.

25 European Medicines Agency. Guideline on the evaluation of the pharmacokinetics of medicinal products in patients with decreased renal function EMA/CHMP/83874/2014. 2014. https://www.ema.europa.eu/en/documents/scientific-guideline/guideline-evaluation-pharmacokinetics-medicinal-products-patients-decreased-renal-function_en.pdf.

26 Trang M, Seroogy JD, Van Wart SA *et al*. Population pharmacokinetic analyses for plazomicin using pooled data from phase 1, 2, and 3 clinical studies. *Antimicrob Agents Chemother* 2019; **63**: 1–15. doi:10.1128/AAC.02329-18

27 Xuan D, Nicolau DP, Nightingale CH. Population pharmacokinetics of gentamicin in hospitalized patients receiving once-daily dosing. *Int J Antimicrob Agents* 2004; **23**: 291–4. doi:10.1016/j.ijantimicag.2003.07.010

28 Aarons L, Vozeh S, Wenk M *et al*. Population pharmacokinetics of tobramycin. *Br J Clin Pharmacol* 1989; **28**: 305–14. doi:10.1111/j.1365-2125.1989.tb05431.x

29 Romano S, Del Mar Fdez de Gatta M, Calvo V *et al*. Influence of clinical diagnosis in the population pharmacokinetics of amikacin in intensive care unit patients. *Clin Drug Investig* 1998; **15**: 435–44. doi:10.2165/00044011-199815050-00008

30 USCAST, The National Antimicrobial Susceptibility Testing Committee for the United States. Aminoglycoside *in vitro* susceptibility test interpretive criteria evaluations version 1.3. 2019. http://www.uscast.org/.

31 Duong A, Simard C, Wang YL *et al*. Aminoglycosides in the intensive care unit: what is new in population PK modeling? *Antibiot (Basel, Switzerland)* 2021; **10**: 507. doi: 10.3390/antibiotics10050507

32 US FDA. Guidance for industry population pharmacokinetics. 2022. https://www.fda.gov/media/128793/download.

33 Marsot A, Guilhaumou R, Riff C *et al*. Amikacin in critically ill patients: a review of population pharmacokinetic studies. *Clin Pharmacokinet* 2017; **56**: 127–38. doi:10.1007/s40262-016-0428-x

34 Llanos-Paez CC, Hennig S, Staatz CE. Population pharmacokinetic modelling, Monte Carlo simulation and semi-mechanistic pharmacodynamic modelling as tools to personalize gentamicin therapy. *J Antimicrob Chemother* 2017; **72**: 639–67. doi: 10.1093/jac/dkw461

35 Krause KM, Serio AW, Kane TR *et al*. Aminoglycosides: an overview. *Cold Spring Harb Perspect Med* 2016; **6**: a027029. doi:10.1101/cshperspect.a027029

36 Simon VK, Mösinger EU, Malerczy V. Pharmacokinetic studies of tobramycin and gentamicin. *Antimicrob Agents Chemother* 1973; **3**: 445–50. doi:10.1128/AAC.3.4.445

37 Cass RT, Brooks CD, Havrilla NA *et al*. Pharmacokinetics and safety of single and multiple doses of ACHN-490 injection administered intravenously in healthy subjects. *Antimicrob Agents Chemother* 2011; **55**: 5874–80. doi:10.1128/AAC.00624-11

38 Pea F, Viale P, Furlanut M. Antimicrobial therapy in critically ill patients: a review of pathophysiological conditions responsible for altered disposition and pharmacokinetic variability. *Clin Pharmacokinet* 2005; **44**: 1009–34. doi:10.2165/00003088-200544100-00002

39 Levey AS, Stevens LA, Schmid CH *et al*. A new equation to estimate glomerular filtration rate. *Ann Intern Med* 2009; **150**: 604–12. doi:10.7326/0003-4819-150-9-200905050-00006

40 Mould DR, Upton RN. Basic concepts in population modeling, simulation, and model-based drug development. *CPT Pharmacometrics Syst Pharmacol* 2012; **1**: e6. doi:10.1038/psp.2012.4

41 Rayner CR, Smith PF, Andes D *et al*. Model-informed drug development for anti-infectives: state of the art and future. *Clin Pharmacol Ther* 2021; **109**: 867–91. doi:10.1002/cpt.2198

42 Holbrook SYL, Garneau-Tsodikova S. Evaluation of aminoglycoside and carbapenem resistance in a collection of drug-resistant Pseudomonas aeruginosa clinical isolates. *Microb Drug Resist* 2018; **24**: 1020–30. doi:10.1089/mdr.2017.0101

43 Leggett JE, Fantin B, Ebert S *et al*. Comparative antibiotic dose-effect relations at several dosing intervals in murine pneumonitis and thigh-infection models. *J Infect Dis* 1989; **159**: 281–92. doi:10.1093/infdis/159.2.281